

Observation of a Significantly Reduced $^1J_{C-H}$ Coupling Constant in an Agostic f-Element Complex: X-ray Crystal Structure of $(ArO)Sm[(\mu-OAr)(\mu-Me)AlMe_2]_2$ (Ar = 2,6-*i*-Pr₂C₆H₃)

John C. Gordon,^{*,1a} Garth R. Giesbrecht,^{1b} John T. Brady,^{1a} David L. Clark,^{1c}
D. Webster Keogh,^{1d} Brian L. Scott,^{1a} and John G. Watkin^{1a}

Chemistry (C) Division, Nuclear Materials Technology (NMT) Division and the Glenn T. Seaborg Institute for Transactinium Science, Los Alamos National Laboratory, Los Alamos, New Mexico 87545

Received July 16, 2001

Reaction of $[Sm(OAr)_3]_2$ with 4 equiv of trimethylaluminum leads to formation of the bis-trimethylaluminum adduct $(ArO)Sm[(\mu-OAr)(\mu-Me)AlMe_2]_2$, which exhibits very short Sm–C(bridging) distances of 2.620(5) and 2.632(5) Å. A reduced $^1J_{C-H}$ coupling constant of 106 Hz and a low $\nu(C-H)$ stretch in the solution and solid-state IR spectrum are indicative of a strong agostic $Sm\cdots H-C$ interaction in solution.

Introduction

It is now widely accepted that metal centers may temper their Lewis acidity by engaging in agostic interactions with the electron-rich C–H bonds of proximal ligands.² Although many examples of agostic $M\cdots H-C$ interactions with transition metal centers have been supported by 1H and ^{13}C NMR data, the paramagnetism of the lanthanide metals (with the exception of lanthanum and lutetium) has precluded detailed NMR studies from being carried out on the analogous f-element species. Thus, the identification of agostic interactions in f-element complexes has been accomplished almost exclusively as a result of the observation of short M–C distances in single-crystal X-ray structure determinations.^{3,4} However, recent detailed studies into the nature of agostic interactions between lanthanide metals and the bulky ligands $-CH(SiMe_3)_2$ ^{5–7} and $-N(SiHMe_2)_2$ ^{8–10} have shed new light upon this subject. Neutron diffraction and DFT studies by Schaverien and co-workers have revealed that the agostic interactions in the lanthanide complexes $(\eta^5-C_5Me_5)La[CH(SiMe_3)_2]_2$ and $(\eta^5-C_5Me_5)Y(O-2,6-t-Bu_2C_6H_3)[CH(SiMe_3)_2]$ are in fact attributable to $\beta-Si-C$ rather than $\alpha-C-H$ or $\gamma-C-H$ interactions with the metal center.⁷ In particular, the following distinctive proper-

ties of these $\beta-Si-C$ agostic systems were noted: (i) neutron diffraction studies revealed no significant differences between agostic and nonagostic C–H bond lengths; (ii) the hydrogens of the agostic methyl groups were staggered with respect to the metal center; and (iii) there was a significant elongation in the Si–C bond of the methyl groups making the agostic interactions (by ca. 0.035 Å). In a more recent paper, however, Anwender et al. reported the observation of more “classical” agostic $\beta-Si-H\cdots Ln$ interactions in a series of lanthanide complexes bearing the $-N(SiHMe_2)_2$ ligand. These systems, of the type *rac*- $[Me_2Si(2-Me-Benz-Ind)_2]Ln[N(SiHMe_2)_2]$, were found to display diagnostic features typical of transition metal agostic interactions, such as reduced $^1J_{Si-H}$ couplings as low as 133 Hz and an infrared Si–H stretch lowered by over 300 cm^{-1} from that observed in the free ligand.⁸ Further theoretical work by Herrmann et al. confirmed the plausibility of partial donation of the Si–H bonding electron pair into a metal sd^2 hybrid orbital and also noted that the reversed polarity in the silicon–hydrogen bond $[(\delta^+)Si-H(\delta^-)]$ compared with the carbon–hydrogen bond $[(\delta^-)C-H(\delta^+)]$ could add a further favorable electrostatic component to the agostic interaction with the electropositive lanthanide metal center.¹¹ Eisenstein has also performed DFT calculations on model $Ln-[N(SiH_3)_2]_3$ systems⁹ and observed significant $Ln\cdots H-Si$ agostic interactions.

Some time ago we reported the isolation of the tetrameric lanthanide neopentoxide complexes $[Ln(OCH_2-t-Bu)_3]_4$ ($Ln = La, Nd$) and demonstrated that they displayed lowered infrared C–H stretching frequencies both in the solid state and in solution, indicative of “classical” $Ln\cdots H-C$ interactions.¹² Here we describe the synthesis and X-ray crystal structure of the heterobimetallic species $(ArO)Sm[(\mu-OAr)(\mu-Me)AlMe_2]_2$

(1) (a) C-SIC, Mail Stop J514. (b) NMT-DO, Mail Stop J514. (c) G. T. Seaborg Institute, Mail Stop E500. (d) C-SIC, Mail Stop G739.

(2) Brookhart, M.; Green, M. L. H.; Wong, L. L. *Prog. Inorg. Chem.* **1988**, *36*, 1.

(3) Nakamura, H.; Nakayama, Y.; Yasuda, H.; Maruo, T.; Kanehisa, N.; Kai, Y. *Organometallics* **2000**, *19*, 5392.

(4) Qian, C.; Nie, W.; Sun, J. *Organometallics* **2000**, *19*, 4134.

(5) van der Heijden, H.; Schaverien, C. J.; Orpen, A. G. *Organometallics* **1989**, *8*, 255.

(6) Schaverien, C. J.; Nesbitt, G. J. *J. Chem. Soc., Dalton Trans.* **1992**, 157.

(7) Klooster, W. T.; Brammer, L.; Schaverien, C. J.; Budzelaar, P. H. M. *J. Am. Chem. Soc.* **1999**, *121*, 1.

(8) Eppinger, J.; Spiegler, M.; Hieringer, W.; Herrmann, W. A.; Anwender, R. *J. Am. Chem. Soc.* **2000**, *122*, 3080.

(9) Maron, L.; Eisenstein, O. *New J. Chem.* **2001**, *25*, 255.

(10) Nagl, I.; Scherer, W.; Tafipolsky, M.; Anwender, R. *Eur. J. Inorg. Chem.* **1999**, 1405.

(11) Hieringer, W.; Eppinger, J.; Anwender, R.; Herrmann, W. A. *J. Am. Chem. Soc.* **2000**, *122*, 11983.

(12) Barnhart, D. M.; Clark, D. L.; Gordon, J. C.; Huffman, J. C.; Watkin, J. G.; Zwick, B. D. *J. Am. Chem. Soc.* **1993**, *115*, 8461.

(Ar = 2,6-*i*-Pr₂C₆H₃) and the identification, by IR and NMR spectroscopy, of significant agostic interactions between the metal center and remote aluminum-bound alkyl groups. Intriguingly, the close Ln–methyl contacts in this molecule are found to display features typical of both a Schaverien-type β -Ln \cdots C–Si agostic system as well as a “classical” γ -Ln \cdots H–C interaction.

Results and Discussion

Reaction of the π -arene-bridged dimer [Sm(OAr)₃]₂ (**1**) (Ar = 2,6-*i*-Pr₂C₆H₃)¹³ with 4 equiv of trimethylaluminum leads to isolation of the bis-trialkylaluminum adduct (ArO)Sm[(μ -OAr)(μ -Me)AlMe₂]₂ (**2**) in good yield (eq 1).

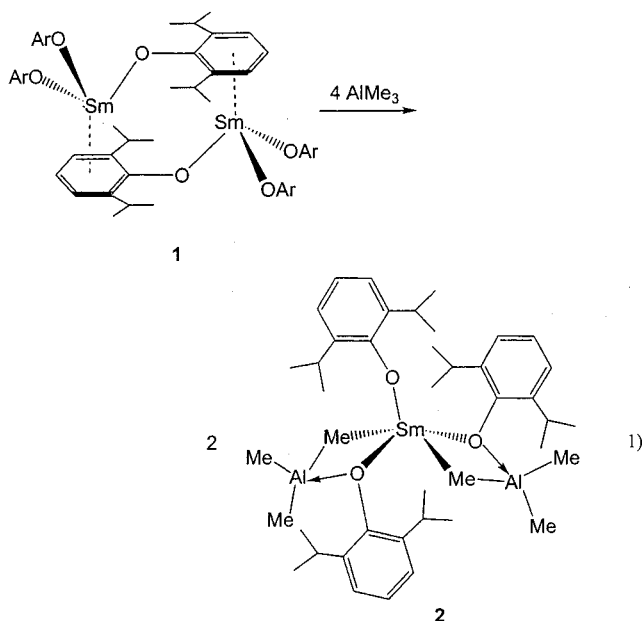


Figure 1. ORTEP view of (ArO)Sm[(μ -OAr)(μ -Me)AlMe₂]₂ (**2**) drawn with 30% probability ellipsoids. Isopropyl methyl groups have been omitted for clarity.

2.75(1) Å found in (η -C₅Me₅)₂Sm[(μ -Me)AlMe₂(μ -Me)]₂-Sm(η -C₅Me₅)₂.¹⁷ The Sm–C bond distances in **2** are also slightly shorter than analogous interactions reported in other complexes displaying bridging Ln[(μ -OR)(μ -Me)]-AlMe₂ units.^{14,18,19}

The hydrogen atoms on C(37) were located and refined during the X-ray crystal structure analysis and reveal a distorted trigonal bipyramidal geometry about this five-coordinate carbon atom, with the samarium center and H(37c) occupying the axial positions; the Sm–C–H(axial) angle is 169(3)°. Notably, the hydrogens on the agostic methyl group are “staggered” with respect to the metal center; that is, none of the C–H bonds point directly toward the samarium. The hydrogen atoms on similarly interacting γ -methyl groups have been reliably located by X-ray diffraction studies in only a handful of cases,⁶ and the trigonal bipyramidal geometries about the pentacoordinate carbon atoms in **2** are somewhat more distorted than those found in (η ⁵-C₅Me₄SiMe₃)Y[(μ -OCMe₃)(μ -Me)AlMe₂]₂¹⁸ or Nd(AlMe₄)₃(Al₂Me₆)_{0.5},²⁰ the latter of which was characterized by neutron diffraction. We also note that there is a distinct elongation in the Al–C bond of the agostic methyl groups; that is, the Al(1)–C(37) distance of 2.060(5) Å is 0.1 Å longer than either of the remaining Al–C bonds (1.945(5) and 1.960(5) Å), and a similar pattern is observed for the methyl groups on Al(2). By way of comparison, the Al–C distances for the terminal methyl groups of Al₂Me₆ average 1.97 Å.²¹

Sm–O distances to the two aluminum-coordinated aryloxo ligands are 2.287(3) and 2.297(3) Å, while that of the unique terminal aryloxo is 2.066(3) Å. These distances compare to those of 2.101(6) and 2.198(5) Å

A single-crystal X-ray diffraction study of **2** revealed an essentially square-based pyramidal geometry about the metal center, with a terminal aryloxo ligand occupying the apical site and two Sm[(μ -OAr)(μ -Me)AlMe₂] moieties in the base (Figure 1). The overall geometry of **2** is closely related to that of (*t*-BuO)-(THF)Y[(μ -O-*t*-Bu)(μ -Me)AlMe₂]₂, which contains a terminal alkoxide ligand and two yttrium–alkoxide linkages which are spanned by AlMe₃ groups.¹⁴ The most noteworthy structural features of **2** are the short Sm–C distances of 2.620(5) and 2.632(5) Å to the bridging alkyl groups.¹⁵ While these distances are longer than terminal samarium–carbon σ -bonds seen in alkyl complexes such as Sm[CH(SiMe₃)₂]₃ (2.33(2) Å)¹⁶ or (η ⁵-C₅Me₅)₂SmMe(THF) (2.484(14) Å),¹⁷ they are considerably shorter than the typical Sm–C(bridging methyl) distance of

(13) Barnhart, D. M.; Clark, D. L.; Gordon, J. C.; Huffman, J. C.; Vincent, R. L.; Watkin, J. G.; Zwick, B. D. *Inorg. Chem.* **1994**, *33*, 3487.

(14) Evans, W. J.; Boyle, T. J.; Ziller, J. W. *J. Am. Chem. Soc.* **1993**, *115*, 5084.

(15) We have also structurally characterized the closely related triethylaluminum adduct (ArO)Sm[(μ -OAr)(μ -Et)AlEt₂]₂ and found equally short Sm–C distances to the bridging methylene groups. Gordon, J. C.; Giesbrecht, G. R.; Brady, J. T.; Clark, D. L.; Keogh, D. W.; Scott, B. L.; Watkin, J. G. Unpublished results.

(16) Hitchcock, P. B.; Lappert, M. F.; Smith, R. G.; Bartlett, R. A.; Power, P. P. *Chem. Commun.* **1988**, 1007.

(17) Evans, W. J.; Chamberlain, L. R.; Ulibarri, T. A.; Ziller, J. W. *J. Am. Chem. Soc.* **1988**, *110*, 6423.

(18) Evans, W. J.; Boyle, T. J.; Ziller, J. W. *J. Organomet. Chem.* **1993**, *462*, 141.

(19) Biagini, P.; Lugli, G.; Abis, L.; Millini, R. *J. Organomet. Chem.* **1994**, *C16*.

(20) Klooster, W. T.; Lu, R. S.; Anwander, R.; Evans, W. J.; Koetzle, T. F.; Bau, R. *Angew. Chem., Int. Ed.* **1998**, *37*, 1268.

(21) Vranka, R. G.; Amman, E. L. *J. Am. Chem. Soc.* **1967**, *89*, 3121.

observed in $[\text{Sm}(\text{OAr})_3]_2$ for the terminal and bridging aryloxy ligands, respectively.¹³ A possible explanation for the very short terminal Sm–O bond distance is that complexation of trimethylaluminum to two aryloxy ligands effectively makes one lone pair on each of these oxygen atoms unavailable for O→M π -bonding and therefore increases the electron deficiency at samarium. To compensate, the terminal ligand engages in very significant π -donation to the metal center, resulting in an almost linear Sm–O–C angle [$\text{Sm}(1)\text{--O}(1)\text{--C}(1) = 173.3(3)^\circ$] and a degree of multiple bond character in the Sm(1)–O(1) linkage.

The ambient-temperature ^1H NMR spectrum of **2** exhibits one broad resonance for the aluminum-bound alkyl groups ($\delta -5.5$ ppm, $\Delta\nu_{1/2} = 50$ Hz), which are undergoing rapid bridge–terminal exchange at this temperature. Lowering the temperature to -90 °C causes a shift of this resonance to higher field, but does not result in decoalescence into separate methyl resonances, as may be expected for a static structure. The room-temperature $^{13}\text{C}\{^1\text{H}\}$ NMR spectrum of **2** also displays a single peak corresponding to the aluminum-bound methyl groups ($\delta -16.0$ ppm, $\Delta\nu_{1/2} = 70$ Hz). The broadness of the peaks resulting from the aluminum-bound methyl groups at all temperatures in the ^1H and ^{13}C NMR spectra can be ascribed to their close proximity to the paramagnetic samarium metal center, and this serves to easily identify peaks arising from carbon atoms and protons in contact with the metal center. When the ^{13}C NMR spectrum of **2** is collected with proton coupling, a broad quartet is observed which displays a significantly reduced $^1J_{C-H}$ coupling constant of 106 Hz; this value was also confirmed by INEPT experiments. Lowering the temperature results in a downfield shift of the ^{13}C resonance to -8.2 ppm ($\Delta\nu_{1/2} = 60$ Hz), but as observed for the variable-temperature ^1H NMR spectra, no decoalescence was observed. This behavior is similar to that reported for $(\eta^5\text{-C}_5\text{Me}_5)_2\text{Yb}(\text{AlEt}_3)(\text{THF})$, which exhibits an unusual Yb($\mu\text{-C}_2\text{H}_5$)Al linkage in the solid state, but only averaged aluminum–ethyl resonances are observed in the variable-temperature ^1H NMR spectra down to -100 °C.²² In contrast, low-temperature $^{13}\text{C}\{^1\text{H}\}$ NMR studies are effective in differentiating the bridge and terminal carbons in Al_2Me_6 even at relatively low field strength.²³ We note that coupling constants of 115 ($^1J_{C-H}$ terminal) and 112 ($^1J_{C-H}$ bridge) Hz have been reported for Al_2Me_6 itself.²³

Despite the fact that bridge–terminal exchange of the aluminum-bound methyl groups in **2** could not be frozen out, the significantly reduced coupling constant of 106 Hz appears to be consistent with a strong “classical” $\text{Sm}\cdots\text{H}\text{--C}$ agostic interaction. In fact, since the measured value of 106 Hz represents an average of the agostic and nonagostic methyl groups, the true $^1J_{C-H}$ coupling determined for the agostic methyl group alone in a frozen-out structure would be expected to be significantly lower than this. Similar $^1J_{C-H}$ values have been noted for the trimethylsilyl groups of $(\eta^5\text{-C}_5\text{Me}_5)\text{-La}[\text{CH}(\text{SiMe}_3)_2]_2(\text{THF})$,⁵ $(\eta^5\text{-C}_5\text{Me}_5)\text{Ce}[\text{CH}(\text{SiMe}_3)_2]_2$,²⁴ and $(\eta^5\text{-C}_5\text{Me}_5)_2\text{Ce}[\text{CH}(\text{SiMe}_3)_2]$,²⁵ although the signifi-

cance of these reduced couplings is complicated by the presence of competing $\beta\text{-Si}\text{--C}\cdots\text{Ln}$ interactions.²⁶

The infrared spectrum of **2** (Nujol mull, KBr plates) shows a weak intensity $\nu(\text{C}\text{--H})$ stretch at 2728 cm^{-1} , consistent with the presence of agostic $\text{C}\text{--H}\cdots\text{Ln}$ interactions in the solid state. The IR spectrum of a benzene solution revealed a similar absorption feature at 2730 cm^{-1} , indicating that an agostic interaction is maintained in solution and consistent with the NMR data. While agostic interactions have been proposed for a variety of f-element complexes on the basis of X-ray crystallography, supporting spectroscopic evidence has usually come in the form of lowered C–H stretching frequencies in solid-state infrared spectra.^{17,18,24} The observation of a lowered C–H stretching frequency in the solution IR spectrum and a significantly reduced $^1J_{C-H}$ coupling constant in the ^{13}C NMR spectrum of **2** indicate that a strong $\text{Sm}\cdots\text{H}\text{--C}$ interaction is maintained in solution.

It can be seen, therefore, that complex **2** displays a contradictory array of spectroscopic data which do not conclusively establish the exact nature of the samarium–methyl group interactions. The staggered hydrogen atoms on the agostic methyl groups and the elongated Al–C bond are features that support a $\beta\text{-Al}\text{--C}\cdots\text{Ln}$ type of interaction in which electron density from the aluminum–carbon bond serves to satisfy the highly electrophilic metal center. However, the reduced C–H coupling constant and the lowered infrared stretching frequencies observed both in the solid state and in solution are characteristic of a “classical” $\gamma\text{-C}\text{--H}\cdots\text{M}$ agostic interaction of the type commonly seen in the d-block transition metals. We also note that the close $\text{Sm}\cdots\text{C}$ contacts of $2.626(6)$ Å (av) in **2** are fully 0.3 Å shorter than the $\text{Ln}\cdots\text{C}$ contacts in the bis(trimethylsilyl)methyl complexes investigated by Schaverien⁷ and that such close $\text{Ln}\cdots\text{C}$ interactions have been observed only in other alkylaluminum adducts of lanthanide alkyl, amido, or alkoxide moieties.^{27–30} To assess whether the steric requirements of the $-\{(\mu\text{-OAr})(\mu\text{-Me})\text{AlMe}_2\}$ ligand were influencing the interactions with the metal center and also to compare the bulk of this ligand with that of bis(trimethylsilyl)methyl and bis(trimethylsilyl)amido ligands, we searched the literature to find a lanthanide-bound ligand that would provide a model for the fragment. It was found that Deacon and co-workers have reported the synthesis and X-ray crystal structures of the lanthanide(II) complexes $\text{Ln}[\text{N}(\text{SiMe}_3)\text{-}2,6\text{-}i\text{-Pr}_2\text{C}_6\text{H}_3]_2(\text{THF})_2$ ($\text{Ln} = \text{Sm}, \text{Yb}$).³¹ Since samarium(II)

(25) Heeres, H. J.; Renkema, J.; Booij, M.; Meetsma, A.; Teuben, J. H. *Organometallics* **1988**, *7*, 2495.

(26) (a) In contrast, the lowering of C–H coupling constants for alkyl groups directly bonded to an f-element metal is quite common.^{5,16,26b–e} (b) Jeske, G.; Schock, L. E.; Swepston, P. N.; Schumann, H.; Marks, T. J. *J. Am. Chem. Soc.* **1985**, *107*, 8103. (c) den Haan, K. H.; de Boer, J. L.; Teuben, J. H.; Spek, A. L.; Kojic-Prodic, B.; Hays, G. R.; Huis, R. *Organometallics* **1986**, *5*, 1726. (d) Schaverien, C. J.; Meijboom, N.; Orpen, A. G. *Chem. Commun.* **1992**, 124. (e) Clark, D. L.; Grumbine, S. K.; Scott, B. L.; Watkin, J. G. *Organometallics* **1996**, *15*, 949.

(27) Evans, W. J.; Anwender, R.; Doedens, R. J.; Ziller, J. W. *Angew. Chem., Int. Ed. Engl.* **1994**, *33*, 1725.

(28) Evans, W. J.; Anwender, R.; Ziller, J. W.; Khan, S. I. *Inorg. Chem.* **1995**, *34*, 5927.

(29) Evans, W. J.; Anwender, R.; Ziller, J. W. *Organometallics* **1995**, *14*, 1107.

(30) Evans, W. J.; Ansari, M. A.; Ziller, J. W. *Inorg. Chem.* **1995**, *34*, 3079.

(31) Deacon, G. B.; Fallon, G. D.; Forsyth, C. M.; Schumann, H.; Weimann, R. *Chem. Ber./Recl.* **1997**, *130*, 409.

(22) Yamamoto, H.; Yasuda, H.; Yokota, K.; Nakamura, A.; Kai, Y.; Kasai, N. *Chem. Lett.* **1988**, 1963.

(23) Yamamoto, O. *J. Chem. Phys.* **1975**, *63*, 2988.

(24) Heeres, H. J.; Meetsma, A.; Teuben, J. H.; Rogers, R. D. *Organometallics* **1989**, *8*, 2637.

is also known to form an analogous bis-THF adduct with the bis(trimethylsilyl)amido ligand, $\text{Sm}[\text{N}(\text{SiMe}_3)_2]_2 \cdot (\text{THF})_2$,³² we conclude that the $-\text{[(}\mu\text{-OAr)(}\mu\text{-Me)AlMe}_2\text{]}_2$ fragment closely matches $-\text{N}(\text{SiMe}_3)_2$ (and presumably $-\text{CH}(\text{SiMe}_3)_2$) in its steric requirements. Interestingly, X-ray crystal structures of the $\text{Ln}[\text{N}(\text{SiMe}_3)_2]_2 \cdot 2,6\text{-}i\text{-Pr}_2\text{C}_6\text{H}_3]_2(\text{THF})_2$ complexes revealed $\text{Ln}\cdots\text{C}$ contacts, but these were weak interactions with the *ipso*-carbons of the aromatic rings rather than with the trimethylsilyl groups.³¹

In conclusion, we have presented structural and spectroscopic data for a complex possessing short $\text{Ln}\cdots\text{methyl}$ group interactions and speculate that the agostic bonding interaction may in fact lie somewhere on a continuum between classical $\text{Ln}\cdots\text{H}-\text{C}$ and the more recently documented $\text{Ln}\cdots\text{C}-\text{X}$ bonding modes ($\text{X} = \text{Si}, \text{Al}$). It is evident, however, that we do not yet have a complete understanding of these bonding schemes and that further detailed studies of a wide range of agostic lanthanide systems will be required in order to fully establish the exact nature of agostic interactions with f-element metal centers.

Experimental Section

General Considerations. All manipulations were carried out under an inert atmosphere of oxygen-free UHP grade argon using standard Schlenk techniques or under oxygen-free helium in a Vacuum Atmospheres glovebox. AlMe_3 (2.0 M hexane solution) was purchased from Aldrich and used as received. $[\text{Sm}(\text{OAr})_3]_2$ ¹³ was prepared according to a literature procedure. Hexane and toluene were deoxygenated by passage through a column of supported copper redox catalyst (Cu-0226 S) and dried by passing through a second column of activated alumina. C_7D_8 was degassed, dried over Na-K alloy, and trap-to-trap distilled before use. ^1H NMR spectra were recorded on a Bruker AMX 500 spectrometer at ambient temperature; chemical shifts are given relative to residual $\text{C}_7\text{D}_7\text{H}$ (2.09 ppm). ^{13}C NMR chemical shifts are given relative to C_7D_8 (20.4 ppm). Infrared spectra were recorded on a Nicolet Avatar 360 FT-IR spectrometer; solid-state spectra were taken as Nujol mulls between KBr plates, while solution spectra were recorded as benzene solutions vs a solvent blank in KBr cells. Elemental analyses were performed on a Perkin-Elmer 2400 CHN analyzer. Elemental analysis samples were prepared and sealed in tin capsules in the glovebox prior to combustion.

(ArO)Sm[(μ -OAr)(μ -Me)AlMe₂]₂ (2). AlMe_3 (0.75 mL of a 2.0 M solution in hexane, 1.50 mmol) was added to a toluene solution of $[\text{Sm}(\text{OAr})_3]_2$ (500 mg, 0.37 mmol). The mixture was stirred at room temperature overnight and then filtered through a Celite pad. The solvent was removed under vacuum, and the sticky residue was washed with a minimum of hexane. Slow evaporation of a saturated toluene solution yielded orange crystals (542 mg, 89% yield). ^1H NMR (500 MHz, C_7D_8): The spectrum consisted of broad, unassignable peaks due to the paramagnetism of the sample. However, the aluminum-methyl peak was upfield of the remaining peaks and was identified on the basis of HMQC experiments: δ -5.5 ppm, $\Delta\nu_{1/2} = 50$ Hz. ^{13}C NMR (125 MHz, C_7D_8): δ -16.0 ppm ($^1J_{\text{C}-\text{H}} = 106$ Hz), $\Delta\nu_{1/2} = 70$ Hz. IR (Nujol, cm^{-1}): 2784 (w), 2728 (w), 1589 (m), 1440 (s), 1382 (s), 1326 (s), 1260 (s), 1203 (s), 1173 (s), 1096 (s), 1045 (s), 937 (m), 891 (s), 866 (s), 840 (s), 804 (m), 753 (s), 697 (s). Anal. Calcd for $\text{C}_{42}\text{H}_{69}\text{Al}_2\text{O}_3\text{Sm}$: C, 61.05; H, 8.42. Found: C, 60.36; H, 8.90.

Crystallographic Studies. A light yellow-orange, rod-shaped crystal was attached to a glass fiber using a spot of

Table 1. Selected Bond Distances (Å) and Angles (deg) for (ArO)Sm[(μ -OAr)(μ -Me)AlMe₂]₂ (2)

Sm1-O1	2.066(3)	Sm1-O2	2.287(3)
Sm1-O3	2.297(3)	Sm1-C37	2.632(5)
Sm1-C40	2.620(5)	O1-C1	1.363(5)
O2-C13	1.405(6)	O3-C25	1.404(4)
O2-Al2	1.891(4)	O3-Al1	1.848(3)
Al1-C37	2.060(5)	Al1-C38	1.945(5)
Al1-C39	1.960(5)	Al2-C40	2.034(5)
Al2-C41	1.950(6)	Al2-C42	1.962(6)
O1-Sm1-O2	118.41(12)	O1-Sm1-O3	118.78(11)
O1-Sm1-C37	101.86(16)	O1-Sm1-C40	101.50(16)
O2-Sm1-O3	122.73(10)	O2-Sm1-C37	94.27(16)
O2-Sm1-C40	72.51(16)	O3-Sm1-C37	71.63(13)
O3-Sm1-C40	98.81(14)	C37-Sm1-C40	156.53(15)
Sm1-O1-C1	173.3(3)	Sm1-O2-C13	125.9(3)
Sm1-O3-C25	135.2(2)	Sm1-O2-Al2	102.75(16)
Sm1-O3-Al1	104.21(11)	Sm1-C37-H37c	169(3)

Table 2. Crystallographic Data for 2

formula	$\text{C}_{42}\text{H}_{69}\text{Al}_2\text{O}_3\text{Sm}$
molecular weight	826.28
temperature, K	203(2)
cryst syst	orthorhombic
space group	$P2_12_12_1$
cryst size, mm	$0.08 \times 0.08 \times 0.08$
a, Å	11.7392(7)
b, Å	18.361(1)
c, Å	20.836(1)
α , deg	90
β , deg	90
γ , deg	90
V, Å ³	4491.1(4)
Z	4
D_{calc} , g/mL	1.222
abs coeff, mm^{-1}	1.379
$F(000)$	1732
θ range, deg	1.5–23.3
total reflns	18 841
ind reflns	6434
GOF	1.187
R1	0.0295
wR2	0.0644

silicone grease. The air-sensitive crystal was mounted from a matrix of mineral oil under argon gas flow. The crystal was immediately placed on a Bruker P4/CCD/PC diffractometer and cooled to 203 K using a Bruker LT-2 temperature device. The data were collected using a sealed, graphite-monochromatized Mo $\text{K}\alpha$ X-ray source. A hemisphere of data was collected using a combination of φ and ω scans, with 20 s frame exposures and 0.3° frame widths. Data collection and initial indexing and cell refinement were handled using SMART³³ software. Frame integration and final cell parameter calculation were carried out using SAINT³⁴ software. The data were corrected for absorption using the SADABS³⁵ program. Decay of reflection intensity was not observed. The structure was solved in space group $P2_12_12_1$ using direct methods and difference Fourier techniques. The initial solution revealed the samarium and the majority of all non-hydrogen atom positions. The remaining atomic positions were determined from subsequent Fourier synthesis. The hydrogen atom positions on one of the agostic carbon atoms, C37, were found on the difference map and refined with isotropic temperature factors set to 0.08 \AA^2 . All other hydrogen atom positions were fixed in ideal positions ($\text{C}-\text{H} = 0.96 \text{ \AA}$ for methyl, 0.97 \AA for methylene, 0.98 \AA for methine, and 0.93 \AA for aromatic). (The hydrogen atom positions on the second agostic carbon atom,

(33) SMART Version 4.210; Bruker Analytical X-ray Systems, Inc.: Madison, WI 53719, 1996.

(34) SAINT Version 4.05; Bruker Analytical X-ray Systems, Inc.: Madison, WI 53719, 1996.

(35) Sheldrick, G. SADABS, first release; University of Göttingen: Germany.

(32) Evans, W. J.; Drummond, D. K.; Zhang, H.; Atwood, J. L. *Inorg. Chem.* **1988**, *27*, 575.

C40, were fixed due to a problematic refinement of the peaks taken from the difference map.) The idealized hydrogen atoms were refined using the riding model, with isotropic temperature factors fixed to 1.5 times (methyl) or 1.2 times (all other) the equivalent isotropic U of the carbon atom they were bound to. The final refinement³⁶ included anisotropic temperature factors on all non-hydrogen atoms and converged with final residuals of $R_1 = 0.0295$ and $wR_2 = 0.0644$. The absolute structure parameter (Flack parameter) refined to 0.005(10). Structure solution, refinement, graphics, and creation of publication materials were performed using SHELXTL NT.³⁷ Additional details of data collection and structure refinement are listed in Table 2.

(36) $R_1 = \sum ||F_o| - |F_c|| / \sum |F_o|$ and $R_{2w} = [\sum [w(F_o^2 - F_c^2)^2] / \sum [w(F_o^2)^2]]^{1/2}$; $w = 1/[\sigma^2(F_o^2) + (aP)^2]$, where $a = 0.0393(2)$, $0.0285(3)$, and $0.0719(4)$.

(37) SHELXTL NT Version 5.10; Bruker Analytical X-ray Instruments, Inc.: Madison, WI 53719, 1997.

Acknowledgment. We acknowledge the Office of Basic Energy Sciences, the Division of Chemical Sciences, and the U.S. Department of Energy for funding (via the LDRD ER program). Los Alamos National Laboratory is operated by the University of California for the U.S. Department of Energy under Contract W-7405-ENG-36.

Supporting Information Available: Listings of fractional atomic coordinates, bond lengths and angles, anisotropic thermal parameters, and hydrogen atom coordinates for complex **2**. This material is available free of charge via the Internet at <http://pubs.acs.org>.

OM010625L